

Degrees of Freedom of the Quark Gluon Plasma, tested by Heavy Mesons

H. Berrebrah, M. Nahrgang, T. Song, V. Ozvenchuck, P.B. Gossiaux, K. Werner,
E. Bratkovskaya and J. Aichelin*

Abstract Heavy quarks (charm and bottoms) are one of the few probes which are sensitive to the degrees of freedom of a Quark Gluon Plasma (QGP), which cannot be revealed by lattice gauge calculations in equilibrium. Due to the rapid expansion of the QGP energetic heavy quarks do not come to an equilibrium with the QGP. Their energy loss during the propagation through the QGP medium depends strongly on the modelling of the interaction of the heavy quarks with the QGP quarks and gluons, i.e. on the assumption of the degrees of freedom of the plasma. Here we compare the results of different models, the pQCD based Monte-Carlo (MC@shQ), the Dynamical Quasi Particle Model (DQPM) and the effective mass approach, for the

H. Berrebrah
FIAS, University of Frankfurt, Ruth Moufang Str.1 60438 Frankfurt, Germany

M. Nahrgang
Department of Physics, Duke University, Durham, North Carolina 27708-0305, USA

T. Song
FIAS, University of Frankfurt, Ruth Moufang Str.1 60438 Frankfurt

V. Ozenchuck
IFJ PAN, Radzikowskiego 152, 31-342 Cracow, Poland

P.B. Gossiaux
SUBATECH, UMR 6457, Université de Nantes, Ecole des Mines de Nantes, IN2P3/CNRS. 4 rue Alfred Kastler, 44307 Nantes cedex 3, France

K. Werner
SUBATECH, UMR 6457, Université de Nantes, Ecole des Mines de Nantes, IN2P3/CNRS. 4 rue Alfred Kastler, 44307 Nantes cedex 3, France

E. Bratkovskaya
GSI Helmholtzzentrum für Schwerionenforschung GmbH, Planckstrasse 1, 64291 Darmstadt, Germany and Institut für Theoretische Physik, Johann Wolfgang Goethe Universität, Max-von-Laue-Str. 1, 60438 Frankfurt am Main, Germany

*J. Aichelin, invited speaker,
SUBATECH, UMR 6457, Université de Nantes, Ecole des Mines de Nantes, IN2P3/CNRS. 4 rue Alfred Kastler, 44307 Nantes cedex 3, France

drag force in a thermalized QGP and discuss the sensitivity of heavy quark energy loss on the properties of the QGP as well as on non-equilibrium dynamics.

1 Introduction

The properties of infinite, strongly interacting systems in thermal equilibrium can presently only be determined by lattice gauge calculations. In recent years the calculations of different groups converged [1, 2] and therefore the pressure, the interaction measure and the entropy density as a function of temperature are known by now. These calculations predict that at high temperature and density the hadrons convert into a plasma of quarks and gluons (QGP). At zero chemical potential the hadronic phase and the QGP phase are separated by a cross over. At finite chemical potentials, where presently the sign problem does not allow for lattice gauge calculations, the transition may be a first order phase transition as several QCD inspired models predict. These lattice calculations do not reveal, however, the degrees of freedom in the QGP or at the transition between hadrons and QGP. The finite value of the interaction measure, $\varepsilon - 3p$, where ε is the energy density and p the pressure, which is zero for a noninteracting gas of Fermions and Bosons, tell us, however, that the constituents interact with each other but the kind of interaction remains unrevealed. On the other hand, these degrees of freedom are essential when we want to study the properties of the QGP beyond thermodynamics. They influence the results if the QGP is tested by probes which do not come to a thermal equilibrium with the QGP. The other way round, the observables of these probes may reveal the degrees of freedom of the QGP or of hadrons close to the phase transition.

There is ample evidence that at top-RHIC and LHC energies during ultrarelativistic heavy-ion collisions a color-deconfined QCD medium of high temperatures and densities, the quark-gluon plasma (QGP), is created. This allows for the first time to study experimentally the properties of this new state of matter, predicted by lattice gauge calculation. To study these properties one needs probes which do not come to a thermal equilibrium with the plasma particles, otherwise all their memory effects on the interaction with the plasma particles are lost.

One of the most promising probes are heavy-flavor quarks which are predominantly produced in the initial hard nucleon-nucleon interactions. Because these collisions are hard they can be calculated by perturbative QCD [3, 4, 5]. Due to the propagation through the colored partonic medium high- p_T heavy quarks suffer from a substantial energy loss, while low- p_T heavy quarks are expected to thermalize at least partially within the medium. The nuclear modification factor, R_{AA} , which is the ratio of the spectra measured in heavy-ion collisions to the scaled proton-proton reference, and the elliptic flow, v_2 , which is at low- p_T a measure of thermalization inside the medium and reflects at high- p_T the spatial anisotropy of the initial state, are presently the most discussed observables of heavy-flavor hadrons and their decay leptons.

A suppression of high- p_T D mesons, heavy-flavor decay electrons and muons has experimentally been measured by the STAR [6, 7] and Phenix [8] collaborations at RHIC as well as the ALICE [9, 10, 11] and CMS [12] collaborations at LHC. Finite values of v_2 of D mesons, heavy-flavor decay electrons and muons was found both at RHIC [13] and at LHC [14].

Perturbative QCD calculations for the average energy loss of high- p_T particles include elastic [15, 16, 17, 18] and/or inelastic scatterings [19, 20, 21, 22, 23, 24, 25, 26, 27, 28, 29, 30, 31, 32]. In most of these models, no evolution of the QGP is considered and only average temperatures and path-length distributions are included. The generic form of the R_{AA} as a function of p_T or the integrated R_{AA} as a function of centrality can easily be reproduced by most calculations on the basis of fundamental principles despite rather different ingredients. The strength of the suppression, however, depends strongly on the details of the space-time evolution of the QGP [33]. For quantitative predictions the fully coupled dynamics of the heavy quarks and of the QGP needs to be taken into account. Therefore we concentrate here on three approaches which have in common that they use not only a Boltzmann collision kernel to describe the interaction of the heavy quark with the plasma particle but as well a dynamical time evolution of the QGP itself.

1) The first of these models is the MC@sHQ approach which assumes that gluons and quarks of the QGP are massless. The interaction of the heavy quark with the plasma particles uses Born type diagrams with a coupling constant depending on the momentum transfer and a hard thermal loop inspired gluon propagator. Here two versions are available, one in which the heavy quarks interact only elastically with the QGP particles and one which includes in addition radiative collisions (i.e. gluon bremsstrahlung). The expansion of the QGP is described by the EPOS event generator.

2) The second approach, dubbed effective mass approach assumes that the gluons and quarks in the entrance and exit channel of the elementary interactions are massive. Their mass is obtained by a fit to the entropy density calculated by lattice gauge calculations.

3) The third model is the PHSD approach which uses the dynamical quasi particle mode (DQPM) to calculate the masses and widths of the plasma constituents as well as temperature dependent coupling constants from a fit to the results of lattice data. Collisions between heavy quarks and light quarks and gluons are here limited to elastic collisions. They are calculated by Born diagrams with "re-summed" propagators and vertexes.

In section 2 we start out with the description of the MC@sHQ approach, section 3 is devoted to the models which treat quarks and gluons as quasiparticles. In section 4 we introduce the drag coefficient and discuss the results obtained for the different models.

2 The standard MC@sHQ approach

In the standard MC@sHQ approach [17, 34] the heavy quarks can interact with the plasma constituents purely elastically or in a combination of elastic and inelastic collisions. The elastic cross sections in Born approximation are obtained within a hard thermal loop (HTL) calculation, including a running coupling constant α_s [35, 17]. The contribution from the t -channel is regularized by a reduced Debye screening mass κm_D^2 , which is calculated self-consistently [17, 18], yielding a gluon propagator with

$$1/Q^2 \rightarrow 1/(Q^2 - \kappa \tilde{m}_D^2(T)) \quad (1)$$

for a momentum transfer Q^2 . In this HTL+semihard approach [17], κ is determined such that the average energy loss is maximally insensitive to the intermediate scale between soft (with a HTL gluon propagator) and hard (with a free gluon propagator) processes. The inelastic cross sections include both, the incoherent gluon radiation [36] and the effect of coherence, i.e. the Landaul-Pomeranchuk-Migdal (LPM) effect [37]. In this approach the incoming light partons are considered as massless. Results for heavy-flavour observables previously obtained within MC@sHQ+EPOS2 [38, 39, 40, 41] considered massless light partons in the QGP.

The fluid dynamical evolution is used as a background providing us with the temperature and velocity fields necessary to sample thermal scattering partners for the heavy quarks. The MC@sHQ approach couples the Monte-Carlo treatment of the Boltzmann equation of heavy quarks (MC@sHQ) [17] to the 3 + 1 dimensional fluid dynamical evolution of the locally thermalized QGP following the initial conditions from EPOS2 [42, 43]. EPOS2 is a multiple scattering approach which combines pQCD calculations for the hard scatterings with Gribov-Regge theory for the phenomenological, soft initial interactions. Jet components are identified and subtracted while the soft contributions are mapped to initial fluid dynamical fields. By enhancing the initial flux tube radii viscosity effects are mimicked, while the subsequent 3 + 1 dimensional fluid dynamical expansion itself is ideal. Including final hadronic interactions the EPOS2 event generator has successfully described a variety of bulk and jet observables, both at RHIC and at LHC [42, 43]. For details we refer to the references.

Including elastic and inelastic collisions this approach reproduces quite well the experimental D-meson and non photonic electron data at RHIC and LHC. As an example we display in Fig. 1 the D meson R_{AA} as dashed line, for elastic (coll) as well as for elastic+inelastic collisions (coll+rad) in comparison with ALICE data. Elastic cross sections alone give not sufficient stopping in this approach.

3 Quarks and Gluons as Quasiparticles

It is well known that quasiparticle models are able to reproduce the lattice QCD equation of state [44, 45, 46] by assuming effective dispersion relations for non-

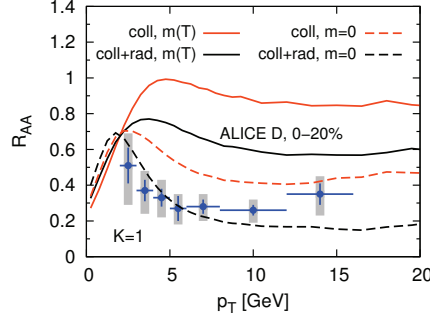


Fig. 1 (Color online) Comparison of the D meson R_{AA} for a QGP consisting of massive quasi-particles (solid lines) and massless partons (dashed lines). Purely collisional (orange, light) and collisional+radiative(LPM) (black line) energy loss scenarios are shown.

interacting quasi-quarks and -gluons in the QGP. Due to the statistical factor of $\exp[-m/T]$ we expect that in a medium with a given temperature the density of light massive partons is reduced as compared to the density of massless partons, what leads to a reduced scattering rate. Thus the mass of the plasma constituents has an immediate influence on the stopping of energetic heavy quarks during their passage through the QGP, or the other way around, measuring the stopping of heavy quarks allows to conclude on the properties of the quasi particles in the medium.

3.1 The effective mass approach

Our second approach is an extension [47] of the model established in [17] by assuming that the incoming and outgoing light partons, which interact with the heavy quarks, have a finite mass. For this purpose, we treat those as well as long-living quasiparticles.

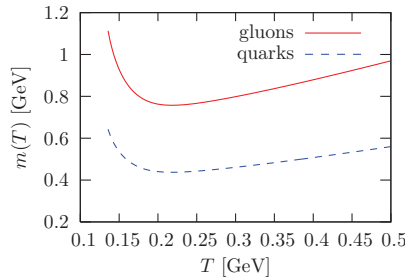


Fig. 2 (Color online) Thermal masses of the quarks and gluons in the QGP within an effective mass approach.

The temperature dependence of the parton masses is obtained from fitting the entropy density of a noninteracting gas of massive quarks and gluons to the lattice equation of state [1, 2].

The pressure and the energy density read

$$p(T) = d_q \int \frac{d^3 p}{(2\pi)^3} \frac{p^2}{3E_q} f_{\text{FD}}(E_q) + d_g \int \frac{d^3 p}{(2\pi)^3} \frac{p^2}{3E_g} f_{\text{BE}}(E_g) - B(T) \quad (2)$$

$$e(T) = d_q \int \frac{d^3 p}{(2\pi)^3} E_q f_{\text{FD}}(E_q) + d_g \int \frac{d^3 p}{(2\pi)^3} E_g f_{\text{BE}}(E_g) + B(T) \quad (3)$$

with $E_q = \sqrt{p^2 + m_q^2}$, $E_g = \sqrt{p^2 + m_g^2}$ and the temperature dependent bag constant $B(T)$. f_{FD} and f_{BE} are the Fermi-Dirac and Bose-Einstein distributions respectively. In order to connect m_q and m_g we use the perturbative HTL-result $m_g = \sqrt{3}m_q$ [48] as a conservative estimate. We assume the same thermal masses for u , d and s quarks. The mean-field contribution B cancels in the entropy density

$$s(T) = \frac{e(T) + p(T)}{T}. \quad (4)$$

The thermal masses of quarks and gluons, obtained by this procedure, are shown in Fig. 2. At high temperatures we find the almost linear behavior as it is known from pQCD calculations. The quasiparticle masses show a strong increase for temperatures above and close to $T = 134$ MeV, which coincides very well with the effective transition temperature T_f from the EPOS parametrization, the transport model which describes the expansion of the QGP in this approach. In this simple quasiparticle picture no assumption about the functional form of the temperature dependence of the thermal masses is made. Other quasiparticle approaches [49, 50] but also the DQPM model, discussed in the next subsection, express the masses via the perturbative form $m^2 \propto g^2 T^2$ and parametrize a logarithmic temperature-dependence of the coupling g by a fit to the lattice QCD equation of state. The definition of the running coupling constant at finite temperatures is not unique. In the effective mass approach one does not assume any explicit temperature dependence of α_s . The coupling is determined by the momentum transfer in the individual scattering process.

A finite mass of the light partons reduces substantially the particle density at a given temperature. Therefore the heavy quarks have less scattering partners and the scattering rate is reduced. A lower scattering rate translates directly into a lower energy loss as can be seen in fig. 1 where the full lines represent the results for the effective mass approach for the same time evolution of the plasma as for the standard MC@sHQ approach.

3.2 The Dynamical QuasiParticle Model (DQPM)

The DQPM describes QCD properties in terms of 'resummed' single-particle Green's functions (in the sense of a two-particle irreducible (2PI) approach). In other words: the degrees-of-freedom of the QGP are interpreted as being strongly interacting massive effective quasi-particles with broad spectral functions (due to the high interaction rates). The dynamical quasiparticle entropy density s^{DQP} has been fitted to lattice QCD calculations which allows to fix for $\mu_q = 0$ the 3 parameters of the DQPM entirely (we refer to the Refs. [44, 51, 52] for the details of the DQPM model).

The DQPM employs a Lorentzian parametrization of the partonic spectral functions $A_i(\omega_i)$, where i is the parton species:

$$\begin{aligned} A_i(\omega_i) &= \frac{\gamma_i}{\tilde{E}_i} \left(\frac{1}{(\omega_i - \tilde{E}_i)^2 + \gamma_i^2} - \frac{1}{(\omega_i + \tilde{E}_i)^2 + \gamma_i^2} \right) \\ &\equiv \frac{4\omega_i\gamma_i}{(\omega_i^2 - \mathbf{p}_i^2 - M_i^2)^2 + 4\gamma_i^2\omega_i^2}, \end{aligned} \quad (5)$$

with $\tilde{E}_i^2(\mathbf{p}_i) = \mathbf{p}_i^2 + M_i^2 - \gamma_i^2$, and $i \in [g, q, \bar{q}, Q, \bar{Q}]$. The spectral functions $A_i(\omega_i)$ are normalized as:

$$\int_{-\infty}^{+\infty} \frac{d\omega_i}{2\pi} \omega_i A_i(\omega_i, \mathbf{p}) = \int_0^{+\infty} \frac{d\omega_i}{2\pi} 2\omega_i A_i(\omega_i, \mathbf{p}_i) = 1,$$

where M_i, γ_i are the dynamical quasi-particle mass (i.e. pole mass) and width of the spectral function for particle i , respectively. They are directly related to the real and imaginary parts of the related self-energy, e.g. $\Pi_i = M_i^2 - 2i\gamma_i\omega_i$, [44]. In the off-shell approach, ω_i is an independent variable and related to the "running mass" m_i by: $\omega_i^2 = m_i^2 + \mathbf{p}_i^2$. The mass (for gluons and quarks) is assumed to be given by the thermal mass in the asymptotic high-momentum regime. We note that this approach is consistent with respect to microcausality in field theory [53]. The DQPM model has originally been designed to reproduce the QCD equation of state, calculated on the lattice, at zero chemical potential μ_q in an effective quasiparticle approach. The fit to the lattice data yields the masses

$$\begin{aligned} M_g^2(T) &= \frac{g^2(T/T_c)}{6} \left((N_c + \frac{1}{2}N_f)T^2 \right), \\ M_q^2(T) &= \frac{N_c^2 - 1}{8N_c} g^2(T/T_c) \left(T^2 \right), \end{aligned} \quad (6)$$

and the widths

$$\gamma_g(T) = \frac{1}{3}N_c \frac{g^2(T/T_c)}{8\pi} T \ln \left(\frac{2c}{g^2(T/T_c)} + 1 \right)$$

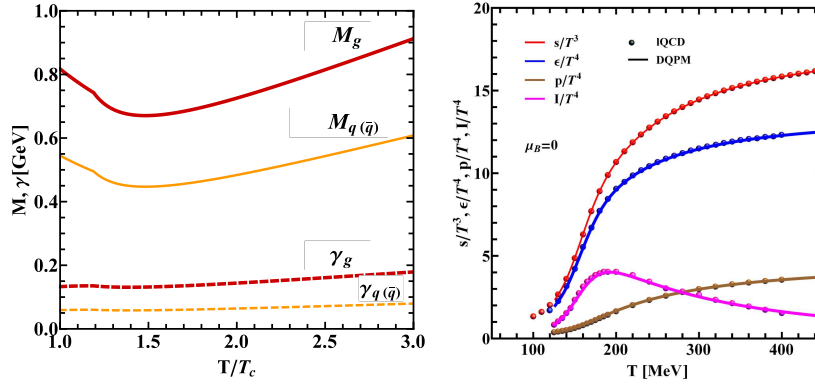


Fig. 3 (Color online) Left: The effective gluon mass M_g and width γ_g as function of the scaled temperature T/T_c (red lines). The blue lines show the corresponding quantities for quarks. Right: The scaled entropy density $s(T)/T^3$ (blue line) and scaled energy density $\epsilon(T)/T^4$ (red line) from the DQPM in comparison to the IQCD results (full dots and triangles).

$$\gamma_q(T) = \frac{1}{3} \frac{N_c^2 - 1}{2N_c} \frac{g^2(T/T_c)}{8\pi} T \ln \left(\frac{2c}{g^2(T/T_c)} + 1 \right). \quad (7)$$

The masses and widths as a function of the scaled temperature are displayed in Fig. 3 (left). We see that the mass of the quasiparticles has a minimum around $1.5 T_c$ and increases at lower and higher temperatures where the increase is linear corresponding to the perturbative thermal Debye mass. The last fit parameter is the coupling constant for which one obtains

$$g^2(T/T_c) = \frac{48\pi^2}{(11N_c - 2N_f) \ln \left(\lambda^2 \left(\frac{T}{T_c} - \frac{T_s}{T_c} \right)^2 \right)} \quad T > T^* = 1.19 T_c,$$

$$g^2(T/T_c) \rightarrow g^2(T^*/T_c) \left(\frac{T^*}{T} \right)^{3.1} \quad T < T^* = 1.19 T_c. \quad (8)$$

with $\lambda = 2.42$, $c=14.4$ and $T_s = 73$ MeV. Eqs. (8) and (7) define the DQPM ingredients necessary for the calculations at finite temperature. In this article we limit ourselves to on-shell quarks and gluons because we have found in Ref. [54] that a finite width $\gamma_{g,q,Q}$ for gluons g , light q and heavy quarks Q has an impact of about 10-20% on the heavy-quark transport coefficients. With this set of fit parameters one obtains an excellent reproduction of the lattice data as one can see in Fig. 3, right.

Based on the Kadanoff Baym equations, with these ingredients a transport theory, the parton hadron string dynamics (PHSD), has been developed which can describe a multitude of observables in ultrarelativistic heavy ion collisions. In particular these masses and coupling constants enter the Boltzmann collision integral in which the scattering is treated in Born approximation. For details we refer again to the Refs [44, 51, 52]. This model describes the heavy quark observables at RHIC [55] and

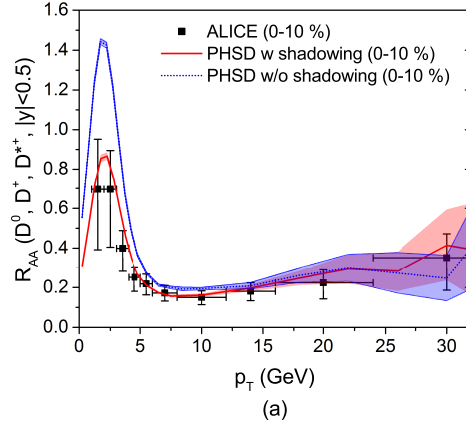


Fig. 4 (Color online) The ratio R_{AA} of D^0 , D^+ , and D^{*+} mesons within $|y| < 0.5$ as a function of p_T in 0-10 % central Pb+Pb collisions at $\sqrt{s_{NN}} = 2.76$ TeV [56] compared with the experimental data from the ALICE collaboration. The solid and dotted lines are, respectively, R_{AA} with and without (anti-)shadowing. The charm quark mass is taken to be 1.5 GeV.

LHC [56] energies. As an example we display in Fig. 4 the calculation for Pb+Pb in comparison with the experimental data **at the LHC**.

4 The Drag coefficient

How can one compare three models, which have a multitude of different ingredients and which give nevertheless quite similar results when compared to the experimental data? The comparison of cross sections themselves (which are a function of the momentum transfer, of the momentum of the scattering partner, of the temperature of the QGP and of the different channels which are considered) is not sufficient since one needs to know which temperatures and momentum transfers are important for the time evolution of the QGP. As a first step it is useful to assume an equilibrium situation and to compare transport coefficients. To understand the meaning of the drag force, the transport coefficient which we study here, it is best to start out from the assumption that the time evolution of the heavy-quark distribution function, $f(\mathbf{p}, t)$, in the QGP can be described by a Fokker-Planck/Langevin approach [57, 58, 59, 60, 61, 62, 63],

$$\frac{\partial f(\mathbf{p}, t)}{\partial t} = \frac{\partial}{\partial p_i} \left[A_i(\mathbf{p}) f(\mathbf{p}, t) + \frac{\partial}{\partial p_j} B_{ij}(\mathbf{p}) f(\mathbf{p}, t) \right]. \quad (9)$$

The interaction of a heavy quark with the QGP is expressed by a drag force A_i and a diffusion tensor B_{ij} , which can be written as B_{\perp} and B_{\parallel} . These quantities can be calculated from the microscopic $2 \rightarrow 2$ processes by

$$\begin{aligned}
\frac{dX}{dt} &= \frac{1}{2E} \int \frac{d^3k}{(2\pi)^3 2E_k} \int \frac{d^3k'}{(2\pi)^3 2E_{k'}} \int \frac{d^3p'}{(2\pi)^3 2E'} \\
&\times \sum_i \frac{1}{d_i} |\mathcal{M}_{i,2 \rightarrow 2}|^2 n_i(k) X \\
&\times (2\pi)^4 \delta^{(4)}(p+k-p'-k'),
\end{aligned} \tag{10}$$

where $p(p')$ and $E = p_0$ ($E' = p'_0$) are momentum and energy of the heavy quark before (after) the collision and $k(k')$ and $E_k = k_0$ ($E_{k'} = k'_0$) are momenta and energies of the colliding light quark ($i = q$) or gluon ($i = g$). For the scattering process of a heavy quark with a light quark ($qQ \rightarrow qQ$) $d_q = 4$ and for the scattering off a gluon ($gQ \rightarrow gQ$) $d_g = 2$. $n_i(k)$ is the thermal distribution of the light quarks or gluons. \mathcal{M}_i is the matrix element for the scattering process i , calculated using pQCD Born matrix elements. In order to calculate the quantities mentioned above, A_i and B_{ij} , one has to take $X = p - p'_i$ and $X = 1/2(p - p'_i)(p - p'_j)$.

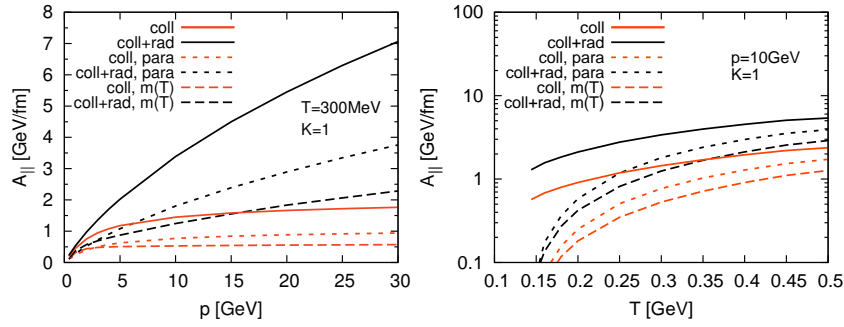


Fig. 5 (Color online) The drag force of c-quarks in the plasma rest frame for three different representations of the QGP constituents: massless partons (solid), EPOS parametrization of the equation of state (short dashed) and massive quasiparticles (long dashed), as a function of the momentum (left) and as a function of the medium temperature (right) [47]. Results for the purely collisional energy loss (black) and for the collisional+radiative(LPM) are shown.

Usually, the simultaneous calculation of both coefficients from Eq. 10 does not satisfy the Einstein relation which assures that asymptotically $f(\mathbf{p}, t)$ is the distribution function at thermal equilibrium. In most Fokker-Planck/Langevin approaches one quantity is calculated and the other one is obtained via the Einstein relation under the assumption that $B_{\perp} = B_{\parallel}$. It has recently been shown that the results from the Fokker-Planck/Langevin approach differ substantially from that of the Boltzmann equation in which the collision integrals are explicitly solved [64] because the underlying assumption, that the scattering angles and the momentum transfers are small, is not well justified. A recent review article [65] gives a broad overview over the various approaches of heavy-flavor energy loss using either the Fokker-Planck/Langevin or the Boltzmann dynamics.

From Eq. (10) one sees immediately that all quantities depend on the distribution of the partonic scattering partners $n_i(k)$. In a thermal medium $n_i(k)$ is given by the

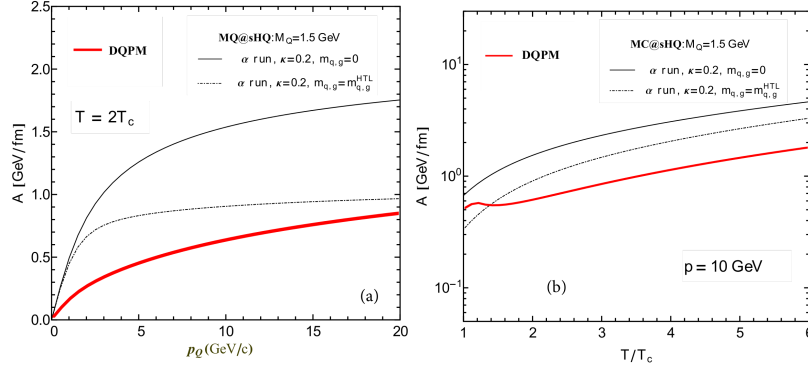


Fig. 6 (Color online) The drag force A of c -quarks in the plasma rest frame for three different approaches as a function of the heavy quark momentum p_Q for $T = 2T_c$ (a) and as a function of the temperature T/T_c ($T_c = 0.158$ GeV) for an intermediate heavy quark momentum, $p_Q = 10$ GeV (b) [54].

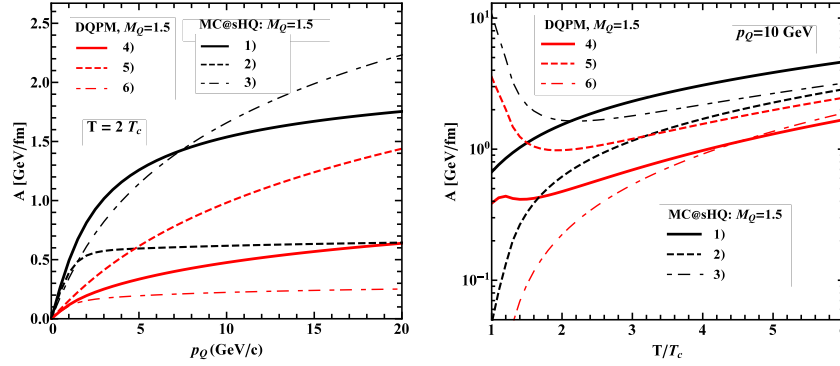


Fig. 7 Drift coefficient A of a heavy quark in a QGP of $T = 2T_c$ for different assumptions of particle masses and coupling constants (see text and Table 1).

Fermi-Dirac, Bose-Einstein or (if quantum statistics is neglected) the Boltzmann distribution. It is obvious that these quantities depend on the local temperature and velocities of the medium, which in the first two approaches are given by a fluid dynamical description of the QGP. In the third approach the evolution is given by the solution of the Kadanoff Baym equations. As a consequence, final observables like R_{AA} and v_2 are strongly affected by the details of the medium evolution. While the solution of the fluid dynamical conservation equations requires only the knowledge of thermodynamic quantities, such as the equation of state and transport coefficients, the actual nature of the quasiparticles is important for the scattering cross sections between heavy quarks and light partons. Even if the Fokker-Planck/Langevin approach does not allow for qualitative comparisons with the data, the drag force is an effective way to compare the stopping of heavy quarks in different transport ap-

	coupling	mass in gluon propagator	mass in external legs
1)	$\alpha(Q^2)$ (ref. [17])	$\kappa = 0.2, m_D$ (eq.1)	$m_{q,g} = 0$
2)	$\alpha(Q^2)$ (ref. [17])	$\kappa = 0.2, m_D$ (eq.1)	$m_{q,g} = m_{q,g}^{DQPM}$ (eq. 8)
3)	$\alpha(T)$ (eq. 7)	$\kappa = 0.2, m_D$ (eq.1)	$m_{q,g} = 0$
4)	$\alpha(T)$ (eq. 7)	m_g^{DQPM} (eq. 8)	$m_{q,g} = m_{q,g}^{DQPM}$ (eq. 8)
5)	$\alpha(T)$ (eq. 7)	m_g^{DQPM} (eq. 8)	$m_{q,g} = 0$
6)	$\alpha(Q^2)$ (ref. [17])	m_g^{DQPM} (eq. 8)	$m_{q,g} = m_{q,g}^{DQPM}$ (eq. 8)

Table 1 Coupling constant, gluon masses in the gluon propagator and the masses of the partons in the external legs of the Feynman diagrams for the different curves shown in Fig.7.

proaches by reducing the complex kinematics to a function which depends on the temperature and the momentum of the heavy quark only.

5 Comparison of the Drag Force for the Different Approaches

As we have seen, the DQPM embedded in the time evolution of the Kadanoff Baym equation describes very well the experimental data, Fig. 4, whereas the effective mass model, Fig. 1, fails. This is astonishing because the masses of the quarks and gluons are rather similar (Fig. 2 and Fig. 3) and both approaches use Born type diagrams for the interaction of the heavy quarks with the light QGP constituents. On the other hand the MC@sHQ, using massless QGP constituents reproduces the data. To elucidate this problem we calculate the drag force for all of the three approaches. In Fig. 5 we compare the drag force of MC@sHQ approach with the effective mass model, in Fig. 6 with the DQPM. In Fig. 5 we see that for larger momenta the energy loss due to radiation becomes more and more dominant over that due to elastic collisions (coll). We see as well that finite masses ($m(T)$) reduce the drag force by large factor, independent of the momentum of the heavy quark, independent of the kind of collisions and also independent of the temperature of the plasma. For a heavy quark with a momentum of 10 GeV this reduction factor is of the order of 4. This is due to the reduced collision rate caused by a lower density of light quarks and gluons at a given temperature and explains why the MC@sHQ approach with temperature dependent masses fails to describe the data.

The comparison between MC@sHQ and DQPM is presented in Fig. 6. The drag force due to elastic collisions in MC@sHQ is marked by the thin line there. The results of the DQPM is the full red line. Regarding the left hand side we observe that at $T = 2T_c$ the drag force for DQPM is always smaller then that due to elastic collisions in MC@sHQ, independent of the heavy quark momentum. So how it is possible that, applied to an expanding plasma, the total energy loss in both approaches is such that the data are reproduced. A first element of the answer is

given by the right hand side of Fig. 6 which shows the temperature dependence of the drag force for a heavy quark with a momentum of $p = 10 \text{ GeV}$. We see that in the DQPM approach the drag force is rather constant below $T = 2T_c$ whereas in MC@sHQ it decreases strongly when approaching the T_c . What is the origin of this quite different behaviour of both approaches? This can be inferred from Fig.7 whose different curves are explained in Table 1. The curve 1) is the drag force for MC@sHQ, curve 4) represents the standard DQPM calculation. If we assume for the external legs the quarks masses of DQPM but keep the other parameters like in the original MC@sHQ we obtain curve 2). The difference between 1) and 2) allows for the study of the dependence of the drag force on the parton masses. Curve 2) does not differ substantially from the results presented in Fig. 5. This allows to conclude that finite parton masses lead to a reduction of the drag force and that this reduction increases the closer we come to T_c . The form of the drag forces changes completely if replace in MC@sHQ $\alpha(Q^2)$ by the temperature dependence DQPM coupling constant $\alpha(T)$ (curve 3). In the relevant temperature regime for heavy ion reactions the drag force increases now with decreasing T/T_c , means the closer we come to T_c the larger gets the energy loss. If we replace in addition in the gluon propagator the MC@sHQ mass (κm_D) by the PHSD gluon mass (curve 5) we see that over the whole temperature range the drag force gets reduced by an almost constant factor as compared to curve 3). If one finally takes the DQPM model and replaces only the temperature dependent coupling constant $\alpha(T)$ by that of MC@sHQ, which depends on the momentum transfer in the collision $\alpha(Q^2)$, curve 6), and compares this drag force with that of the standard version of the DQPM, curve 4), one sees the enormous influence on the choice of the coupling constant for the drag force and hence to the energy loss of the heavy quarks close to T_c . One can conclude from this study that close to T_c finite parton masses at the external legs reduce the drag force whereas it is increased when employing a temperature dependent coupling constant $\alpha(T)$ instead of $\alpha(Q^2)$. The combination of the DQPM coupling constant and the DQPM masses yields to a less steep decrease of the coupling constant when the temperature approaches T_c as compared to MC@sHQ.

Thus MC@sHQ and PHSD (DQPM) display a quite different scenario for the the momentum loss of heavy quarks an a thermal system. In the MC@sHQ approach the energy loss is much stronger when the plasma is hot as compared to that close to T_c . This means that the energy loss takes dominantly place at the beginning of the expansion whereas in the DQPM approach it is opposite. There close to T_c the energy is almost as large as at high T. It has, however, to be mention that the drag force in DQPM is for all temperatures lower than the drag for in MC@sHQ for elastic collisions only. This means that the nonequilibrium effect which are present in PHSD but not in MC@sHQ have a very strong influence on the energy loss.

6 Summary

Heavy quarks have been identified as a tool to study the effective degrees of freedom of the QGP. We have studied here three different approaches - pQCD based MC@sHQ, Dynamical QuasiParticle Model (DQPM) and effective mass approach - where in the last two of them the properties of QGP degrees of freedom (quarks and gluons) are obtained by fitting lattice QCD data. We have shown that the presently available experimental data on R_{AA} of D-mesons can be described by the dynamical models (hydro type or transport approach) based on these different propositions of the effective degrees of freedom. That is in spite of strong sensitivity of the drag force to the model assumptions: finite parton masses and a temperature dependent coupling constant for the heavy quark - light parton collisions modify the drag force in opposite direction, so from momentum loss measurement alone it will be difficult to disentangle both. In addition, models with a coupling constant which depends on the momentum transfer show the strongest momentum loss at the beginning of the expansion whereas in those with temperature dependence coupling constant the momentum loss is shifted towards T_c . In addition, non-equilibrium effects have a strong influence and increase the energy loss of heavy quarks substantially. It will be subject to a future study to explore this in detail.

Acknowledgements This work was supported by BMBF, by the LOEWE center HIC for FAIR” and by the project ”Together” of the region Pays de la Loire, France.

References

1. S. Borsanyi, Z. Fodor, C. Hoelbling, S. D. Katz, S. Krieg and K. K. Szabo, *Phys. Lett. B* **730** (2014) 99.
2. A. Bazavov *et al.* [HotQCD Collaboration], *Phys. Rev. D* **90** (2014) 9, 094503.
3. M. Cacciari, M. Greco and P. Nason, *JHEP* **9805** (1998) 007;
4. M. Cacciari, S. Frixione and P. Nason, *JHEP* **0103** (2001) 006;
5. M. Cacciari, S. Frixione, N. Houdeau, M. L. Mangano, P. Nason and G. Ridolfi, *JHEP* **1210** (2012) 137.
6. STAR Collab., *Phys. Rev. Lett.* **98** (2007) 192301; Erratum-ibid. **106** (2011) 159902;
7. X. Dong [STAR Collaboration], *Nucl. Phys. A* **904-905** **2013** (2013) 19c
8. PHENIX Collab., *Phys. Rev. C* **84** (2011) 044905;
9. ALICE Collab., *JHEP* **09** (2012) 112
10. A. Dainese [ALICE Collaboration], arXiv:1212.0995 [nucl-ex].
11. B. Abelev *et al.* [ALICE Collaboration], arXiv:1305.2707 [nucl-ex].
12. CMS Collaboration [CMS Collaboration], CMS-PAS-HIN-15-005.
13. L. Adamczyk *et al.* [STAR Collaboration], arXiv:1405.6348 [hep-ex].
14. J. Adam *et al.* [ALICE Collaboration], *Phys. Lett. B* **753** (2016) 41
15. Bjorken J D, Fermilab preprint Pub-82/59-THY (1982).
16. Peshier A, *Phys. Rev. Lett.* **97** (2006) 212301;
17. P. B. Gossiaux and J. Aichelin, *Phys. Rev. C* **78** (2008) 014904 [arXiv:0802.2525 [hep-ph]].
18. Peigne S and Peshier A, *Phys. Rev. D* **77** (2008) 114017.
19. Gyulassy M and Wang X N, *Nucl. Phys. B* **420** (1994) 583;

20. Wang X N, Gyulassy M, and Plümer M, *Phys. Rev. D* **51** (1995) 3436;
21. Baier R, Dokshitzer Y L, Peigné S, and Schiff D, *Phys. Lett. B* **345** (1995) 277;
22. Baier R, Dokshitzer Y L, Müller A H, Peigné S, and Schiff D, *Nucl. Phys. B* **483** (1997) 291; *Nucl. Phys. B* **484** (1997) 265;
23. Zakharov B G, *JETP Lett.* **63** (1996) 952; *JETP Lett.* **64** (1996) 781; *JETP Lett.* **65** (1997) 615; *JETP Lett.* **73** (2001) 49; *JETP Lett.* **78** (2003) 759; *JETP Lett.* **80** (2004) 617;
24. Gyulassy M, Levai P, and Vitev I, *Phys. Rev. Lett.* **85** (2000) 5535; *Nucl. Phys. B* **571** (2000) 197; *Nucl. Phys. B* **594** (2001) 371;
25. Dokshitzer Y L and Kharzeev D E, *Phys. Lett. B* **519** (2001) 199;
26. Arnold P B, Moore G D, and Yaffe L G, *JHEP* 0011 (2000) 001; *JHEP* 0305 (2003) 051;
27. Armesto N, Salgado C A, and Wiedemann U A, *Phys. Rev. D* **69** (2004) 114003; *Phys. Rev. C* **72** (2005) 064910;
28. B. W. Zhang, E. Wang and X. N. Wang, *Phys. Rev. Lett.* **93** (2004) 072301 [nucl-th/0309040].
29. M. Djordjevic and M. Gyulassy, *Nucl. Phys. A* **733**, 265 (2004), [nucl-th/0310076].
30. M. Djordjevic, M. Gyulassy and S. Wicks, *Phys. Rev. Lett.* **94** (2005) 112301, [hep-ph/0410372].
31. M. Djordjevic and U. Heinz, *Phys. Rev. C* **77** (2008) 024905, [arXiv:0705.3439 [nucl-th]].
32. M. Djordjevic, *Phys. Rev. C* **80** (2009) 064909 [arXiv:0903.4591 [nucl-th]].
33. T. Renk, *Phys. Rev. C* **85** (2012) 044903 [arXiv:1112.2503 [hep-ph]].
34. J. Aichelin, P. B. Gossiaux and T. Gousset, *Phys. Rev. D* **89** (2014) 7, 074018 [arXiv:1307.5270 [hep-ph]].
35. A. Peshier, hep-ph/0601119.
36. J. F. Guion and G. Bertsch, *Phys. Rev. D* **25** (1982) 746.
37. P. B. Gossiaux, *Nucl. Phys. A* **910-911** (2013) 301 [arXiv:1209.0844 [hep-ph]].
38. M. Nahrgang, J. Aichelin, S. Bass, P. B. Gossiaux and K. Werner, *Phys. Rev. C* **91** (2015) no.1, 014904 doi:10.1103/PhysRevC.91.014904 [arXiv:1410.5396 [hep-ph]].
39. M. Nahrgang, J. Aichelin, S. Bass, P. B. Gossiaux and K. Werner, *Nucl. Phys. A* **931** (2014) 575 doi:10.1016/j.nuclphysa.2014.08.094 [arXiv:1409.1464 [hep-ph]].
40. M. Nahrgang, J. Aichelin, P. B. Gossiaux and K. Werner, *Phys. Rev. C* **89** (2014) no.1, 014905 doi:10.1103/PhysRevC.89.014905 [arXiv:1305.6544 [hep-ph]].
41. M. Nahrgang, J. Aichelin, P. B. Gossiaux and K. Werner, *Phys. Rev. C* **90** (2014) no.2, 024907 doi:10.1103/PhysRevC.90.024907 [arXiv:1305.3823 [hep-ph]].
42. K. Werner, I. Karpenko, T. Pierog, M. Bleicher and K. Mikhailov, *Phys. Rev. C* **82** (2010) 044904
43. K. Werner, I. Karpenko, M. Bleicher, T. Pierog and S. Porteboeuf-Houssais, *Phys. Rev. C* **85** (2012) 064907
44. W. Cassing and E. L. Bratkovskaya, *Nucl. Phys. A* **831**, 215 (2009).
45. M. Bluhm, B. Kampfer and G. Soff, *Phys. Lett. B* **620** (2005) 131 [hep-ph/0411106].
46. H. Berrehrh, E. Bratkovskaya, W. Cassing, P. B. Gossiaux, J. Aichelin and M. Bleicher, *Phys. Rev. C* **89**, no. 5, 054901 (2014) doi:10.1103/PhysRevC.89.054901 [arXiv:1308.5148 [hep-ph]].
47. M. Nahrgang, J. Aichelin, P. B. Gossiaux and K. Werner, arXiv:1602.03544 [nucl-th].
48. M. H. Thoma, In *Hwa, R.C. (ed.): Quark-gluon plasma, vol. 2*, 51-134 and references therein.
49. A. Peshier, B. Kampfer and G. Soff, *Phys. Rev. D* **66** (2002) 094003
50. M. Bluhm, B. Kampfer, R. Schulze and D. Seipt, *Eur. Phys. J. C* **49** (2007) 205 [hep-ph/0608053].
51. W. Cassing, *Eur. Phys. J. ST* **168**, 3 (2009).
52. W. Cassing, *Nucl. Phys. A* **791**, 365 (2007).
53. L. Rauber and W. Cassing, *Phys. Rev. D* **89**, 065008 (2014).
54. H. Berrehrh, P. B. Gossiaux, J. Aichelin, W. Cassing and E. Bratkovskaya, *Phys. Rev. C* **90** (2014) no.6, 064906 doi:10.1103/PhysRevC.90.064906 [arXiv:1405.3243 [hep-ph]].
55. T. Song, H. Berrehrh, D. Cabrera, J. M. Torres-Rincon, L. Tolos, W. Cassing and E. Bratkovskaya, *Phys. Rev. C* **92** (2015) no.1, 014910 doi:10.1103/PhysRevC.92.014910 [arXiv:1503.03039 [nucl-th]].

56. T. Song, H. Berrebrah, D. Cabrera, W. Cassing and E. Bratkovskaya, Phys. Rev. C **93** (2016) no.3, 034906 doi:10.1103/PhysRevC.93.034906 [arXiv:1512.00891 [nucl-th]].
57. B. Svetitsky Phys. Rev. D **37**, 2484 (1988)
58. G. D. Moore and D. Teaney, Phys. Rev. C **71** 064904 (2005).
59. H. van Hees and R. Rapp, Phys. Rev. C **71**, 034907 (2005). [arXiv:nucl-th/0412015].
60. H. van Hees, V. Greco and R. Rapp Phys. Rev. C **73**, 034913 (2006) [arXiv:nucl-th/0508055]
61. V. Greco, H. van Hees and R. Rapp arXiv:0709.4452 [hep-ph]
62. M. He, R. J. Fries and R. Rapp, Phys. Rev. C **86** (2012) 014903 [arXiv:1106.6006 [nucl-th]].
63. S. Cao, G. -Y. Qin and S. A. Bass, arXiv:1308.0617 [nucl-th].
64. S. K. Das, F. Scardina, S. Plumari and V. Greco, arXiv:1309.7930 [nucl-th].
65. A. Andronic *et al.*, arXiv:1506.03981 [nucl-ex].